Available online at www.sciencedirect.com
SCIENCE DIRECT®
ELSEVIER
Journal of the European Ceramic Society 25 (2005) 2821–2823
ECERS
www.elsevier.com/locate/jeurceramsoc

Electrical properties of micro-composites SiC–β'SiAlON under high electric fields, in relation to surface morphology

A. Jankowiak, P. Fourcade, P. Blanchart *

GEMH, ENSCI, 47 à 73 avenue Albert Thomas 87065 Limoges France

Available online 31 March 2005

Abstract

This study describes the electrical behaviour of SiC–β'SiAlON granular composite materials under pulsed high electric fields. Such composite materials favour enhanced discharge on surface and the global electric field required for the discharge is very reduced compared with a similar air gap at the same atmosphere pressure. It is shown that the electrical discharge proceeds with successive steps and the most important one is the local ionisation of the air atmosphere. At the macroscopic scale, ionisation mechanisms are approximated to the Paschen's law and at the microscopic scale, breakdown follows the Fowler–Nordheim's law for the enhanced field emission at SiC grain boundaries. The global electrical properties vary against the surface morphology since the number and shape of macroscopic sites for surface ionisation highly influence the breakdown mechanism.

Keywords: Composites; SiAlON; SiC; Surfaces; Electrical breakdown

1. Introduction

Materials for electrical surface discharge are an attractive solution to obtain hot plasma over the surface. They are suitable for gas or liquid ignition at low and high (up to 2 MPa) atmosphere pressure. The surface discharge materials are composite ceramics including micro-scaled but conductive grains embedded in an insulating or semi conductive matrix material. Over the surface, under a high electric field from external electrodes, a breakdown current flow from electronic field emission mechanisms occurring at localized sites on the material surface. In general, it is assumed that field emission is favoured by surface micro protrusions localised at conductive grains. The local electrical field is highly enhanced to attain high value, which is the threshold for this type of field emission to occur.[1]

In this study, we used particle-reinforced ceramic matrix composites with micro-sized SiC grains and β'-SiAlON as matrix phase. Two similar ceramic matrix composites were investigated but with different SiC grain sizes. They were subjected to electrical discharges at high voltage, to form localized plasma over the material surface. To investigate the mechanisms involved, electrical properties were examined with current versus tension characteristics at atmospheric pressure under air. These results were correlated with the topography of material surfaces.

2. Surface topographies

The SiC–β'SiAlON composite material was prepared from powders of SiC (Starck), Si_3N_4 (Starck, M11), Al_2O_3 (Pechiney, P172) and MgO (Prolabo) as sintering additive. Two different SiC grain sizes were used, but the SiC-matrix phase ratio was maintained at 73 vol.%. In this way, we obtained two very similar materials with equivalent physical properties but with different surface roughness. They were referenced as NC1 ($d_{0.5}$: 17.9 μm) and NC2 ($d_{0.5}$: 7.3 μm). Powders were ball milled in water–dispersant solution to attain a precisely adjusted rheology of the slip during mixing and to limit the reduction of size of SiC grains. After drying, powders were shaped by isostatic compaction at 200 MPa in silicon rubber moulds. The preliminary firing stage was at low

* Corresponding author. Tel.: +33 5 55 45 22 11.
E-mail address: p.blanchart@ensci.fr (P. Blanchart).

0955-2219/$ – see front matter © 2005 Elsevier Ltd. All rights reserved.
doi:10.1016/j.jeurceramsoc.2005.03.148

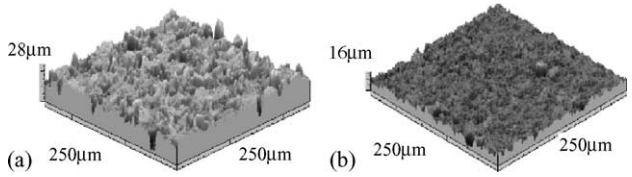

Fig. 1. Surface maps of NC1 (a) and NC2 (b) samples, for 250 μm × 250 μm surfaces.

temperature (500 °C) under vacuum, and the sintering stage was in a graphite kiln at 1680 °C, under N_2 at atmospheric pressure.

Surface topographies were measured on NC1 and NC2 materials by a non-contact optical profiler (NOP) (Fogale Nanotech). In NOP,[2] surface height variations are measured by optical phase shifting and white light vertical scanning interferometry, with a vertical measurement performance of 2 nm. Along the material surface, the light intensity of optical fringes is related to the surface profile and discredited into the measurement array of a camera. Within individual pixel and for each sampling interval, the light intensity represents the averaged value the surface heights within the elementary surface. The lateral spatial sampling is fixed by the magnification of the optical system. We used an objective lens magnification of 10 and the sampling interval is 1 μm in both directions. Surface maps of NC1 and NC2 materials are shown in Fig. 1(a) and (b), respectively.

Roughness (short waves) and waviness (long wave) of surface profiles must be preliminary separated by a filtering operation, to obtain the reference mean surface. This procedure uses a Gaussian filter whose parameters are adjusted to remove most of the waviness.

On profiles, we computed the material ratio curves (Abott curves), which are the depth distribution from the highest peak d_{ph} versus the bearing ratio. S_{mr} is expressed in percent of the sum of material-filled surfaces S_i to the evaluation surface S_m at a given profile section. It is the distance between the measured intersection level and the reference level:

$$S_{mr} = \frac{1}{S_m} \sum_i S_i \times 100 \quad (1)$$

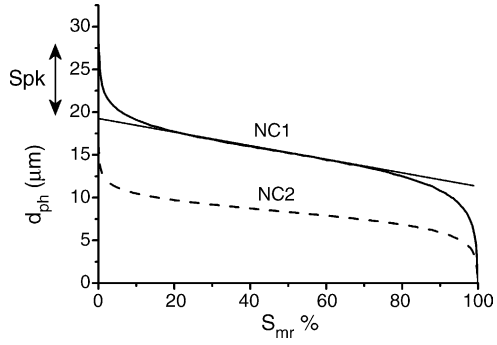

Fig. 2. Abott curves for NC1 and NC2 materials.

Table 1
High spot characteristics

Sample	Peak (mm^{-2})	Mean area (μm^2)	Mean height (μm)
NC1	3876	24.8	3.47
NC2	9922	9.87	1.98

In Fig. 2, Abott curves of NC1 and NC2 samples have similar shapes with a central straight line, which divide the curve in three areas. As the straight-line length is considered to be the depth of the roughness core profile (Fig. 2), S_{pk} is the reduced peak height protruding from the core area. Therefore, we considered that all height values, which are active for the atmosphere ionisation, must be included in the S_{pk} values, i.e. 9 μm for NC1 and 5 μm for NC2. Using this parameter, we calculated the high spot count for each sample, which is the surface density of peaks higher than the material core profile. We calculated also the mean area and the mean heights, which are reported in Table 1. It is seen that surface morphologies of NC1 and NC2 differ significantly since the high spots characteristics are very different.

3. Electrical characteristics of samples

The current–voltage characteristic of our composite material extends to a broad range of voltage and current, about 1200 V and 200 A. The general aspect of curves is presented in Fig. 3 for NC1 and NC2 samples under air atmosphere. In general, a first and rapid increase of voltage is followed by a plateau, where the voltage maximum V_m is attained. The subsequent and very rapid decrease of voltage is accompanied by a large increase of current. During this stage, a second and small voltage characteristic point is observed, followed by a second rapid decrease. During this last stage, hot plasma is formed under the high current density, that it is useful for ignition.

The whole duration of discharges is about 110 μs and the process ends when the capacitor discharge is exhausted. The whole duration of the discharge was adjusted by the capacitance and the damping resistor values placed in series.

It is proposed that the sequence of phenomena can be explained using the knowledge from electric discharges

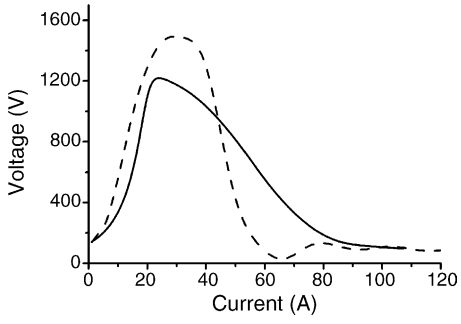

Fig. 3. Current–voltage characteristics for NC1 (straight line) and NC2 (dashed line).

in low-pressure gas, under the Paschen's law. This model reflects the electrical breakdown mechanism in gases at the V_m voltage. V_m is related to the pd product where p is the gas pressure and d is the gap between electrodes:

$$Vm = \frac{Bpd}{\ln(Apd) - \ln(\alpha d)} \quad (2)$$

where A and B are gas dependant parameters. α is the Townsend's first ionisation coefficient, which relates the mean free path for electron secondary ionisation to the total scattering path. It is pressure and electric field dependant. In the continuation of the discharge process, the acceleration of ions in the electric field leads to secondary electron emissions at the electrodes. This secondary emission replenishes the population of ions and the discharge becomes self-sustaining when:

$$\alpha d = \ln\left(1 + \frac{1}{\gamma}\right) \quad (3)$$

where γ is the secondary ionisation coefficient for the electrode surface. When p increases, α decreases from the limiting low-pressure. α is the number of electron-ion pairs generated per unit distance, which is related to the secondary electron emission γ at the cathode through Eq. (3). A large decrease of α means an increase of γ, which exceeds realistic values. Therefore, it is also assumed the occurrence of the Fowler–Nordheim's mechanism.[3] It describes the expression of the current density j flowing between electrodes:

$$j = \frac{aE^2}{\Phi} \exp\left(-b\frac{\Phi^{3/2}}{E}\right) \quad (4)$$

where Φ represents the work function of the material (2.7–5 eV) and E is the electric field. a and b parameters depend on Φ and are estimated as:

$$a = 1.54 \times 10^{-6}\,\mathrm{A\,m^{-2}}, \quad b = 6.83 \times 10^{9}\mathrm{V^{-1/2}m}$$

For our materials, Fowler–Nordheim's law must be modified to take into account the enhanced field emission at local emission sites on surface.[4] Such phenomenon is observed when significant current values exist even for low electric fields. It is supposed that the current emission is enhanced by local microscopic emitting sites as small protrusions. Therefore, the current density j becomes:

$$j = \frac{a\beta^2E^2}{\Phi} \exp\left(-b\frac{\Phi^{3/2}}{\beta E}\right) \quad (5)$$

A linear relationship between $\log(I/E^2)$ and $1/E$ is generally observed during the pre-breakdown voltage period (Fig. 4). The enhancement factor β, calculated from the slope of the characteristic, are 2.1×10^4 for NC1 and 4.3×10^4 for NC2.s

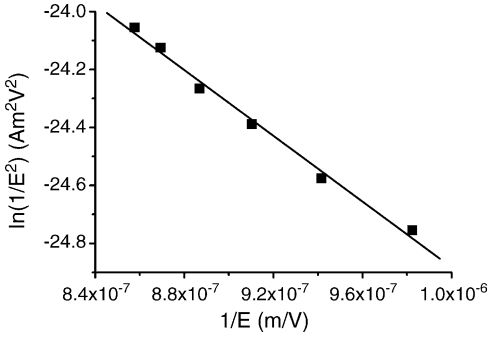

Fig. 4. Fowler–Nordheim plot near the breakdown point.

Such very high values are commonly encountered with carbon or metal films, where small protrusions or thin oxide layers enhance drastically the local electric field.[5]

For both NC1 and NC2 materials β values are not significantly different. It is therefore assumed that material characteristics, at the macroscopic scale, are similar and that the very different electrical responses (Fig. 3) are mainly related to surface topographies.

4. Conclusion

The emission sites on NC1 (SiC $d_{0.5}$: 17.9 μm) surface are significantly coarser but fewer than for NC2 (SiC $d_{0.5}$: 7.3 μm). Besides, β for NC1 is lower than for NC2, whereas V_m for NC1 is reduced in comparison with V_m for NC2. This is explained by surface morphologies of material. For NC1, the mean height of high spots is higher than for NC2, but the number of gaps for current percolation between external electrodes is lower. We suggest that the extended breakdown during the hot plasma event is triggered by a preliminary ionisation process at a limited number of "emitter" sites, whose geometrical and electrical characteristics must be optimised.

References

1. Yuasa, K., Shimoi, A., Ohba, I. and Oshima, C., Modified Fowler–Nordheim field emission formulae from a nonplanar emitter model. *Surf. Sci.*, 2002, **520**(1–2), 18–28.
2. Batalha, G. F. and Stipkovic Filho, M., Quantitative characterization of the surface topography of cold rolled sheets-new approaches and possibilities. *J. Mater. Process. Technol.*, 2001, **113**, 732–738.
3. Lenzlinger, M. and Snow, E. H., Fowler–Nordheim tunneling into thermally grown SiO_2. *J. Appl. Phys.*, 1969, **40**, 278.
4. Evtukh, A. A., Klyui, N. I., Litovchenko, V. G., Litvin, Yu. M., Korneta, O. B., Puzikov, V. M. *et al.*, Peculiarities of field emission from silicon carbide films. *Appl. Surf. Sci.*, 2003, **215**(1–4), 237–241.
5. Obraztsov, A. N., Zakhidov, Al. A., Volkov, A. P. and Lyashenko, D. A., Non-classical electron field emission from carbon materials. *Diamond Relat. Mater.*, 2003, **12**, 446–449.